

The American Journal of Human Genetics, Volume 93

## **Supplemental Data**

### **Global Analysis of DNA Methylation Variation**

#### **in Adipose Tissue from Twins Reveals Links to Disease-**

#### **Associated Variants in Distal Regulatory Elements**

**Elin Grundberg, Eshwar Meduri, Johanna K. Sandling, Åsa K. Hedman, Sarah Keildson,, Alfonso Buil  
Stephan Busche, Wei Yuan, James Nisbet, Magdalena Sekowska, Alicja Wilk, Amy Barrett, Kerrin S. Small,  
Bing Ge, Maxime Caron, So-Youn Shin, the Multiple Tissue Human Expression Resource Consortium, Mark  
Lathrop, Emmanouil T. Dermitzakis, Mark I. McCarthy, Timothy D. Spector, Jordana T. Bell, and Panos  
Deloukas**

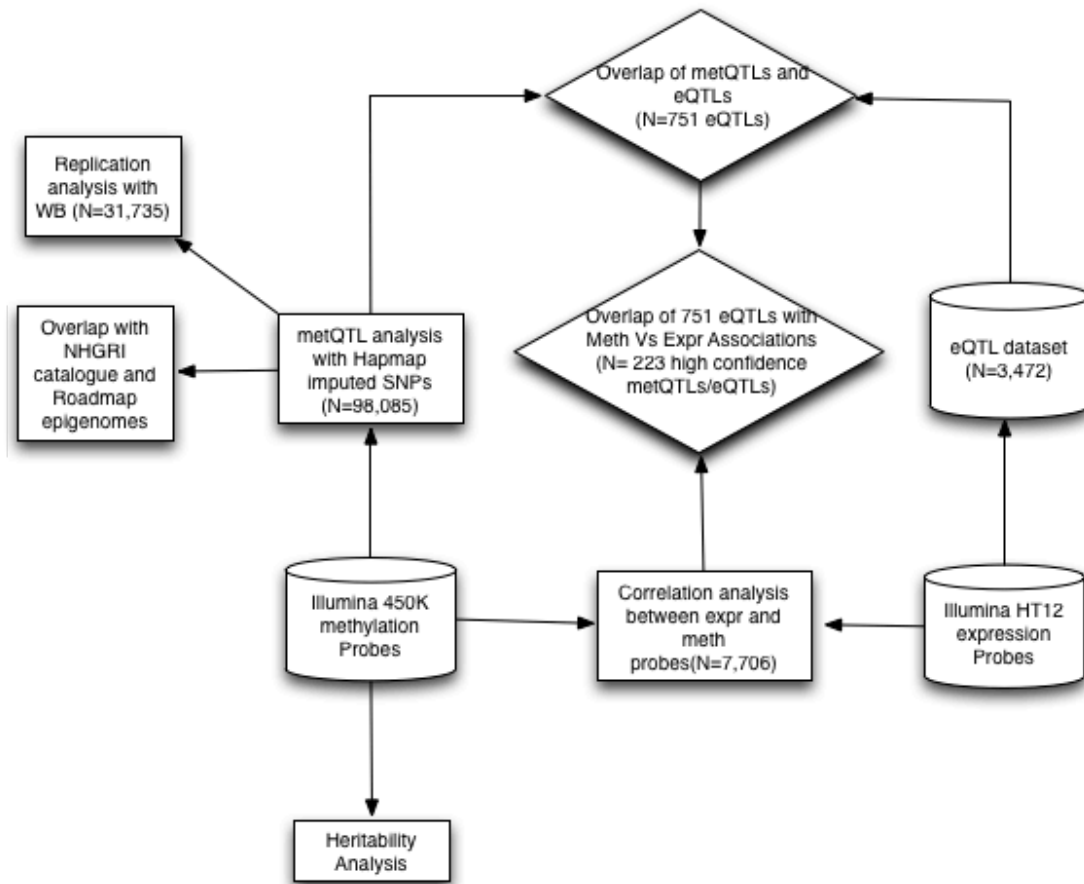


**Figure S1. Analysis pipeline.** Analysis indicated in rectangular boxes was performed on the data shown in cylindrical boxes. Correlation analysis linking different datasets is shown in diagonal boxes. Direction of the arrows represents the workflow of the experimental design. Results at different P-Value cut-offs are indicated in the brackets.

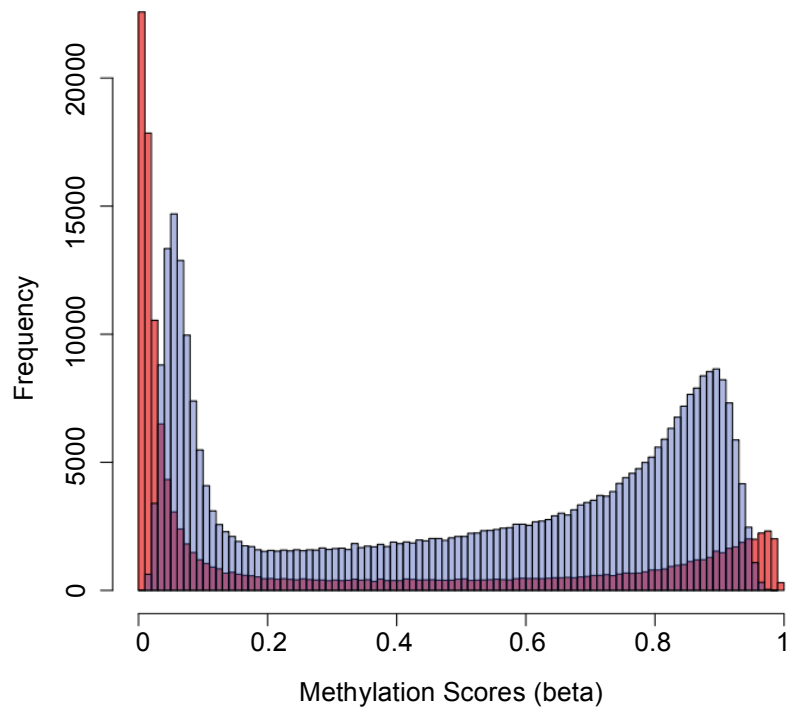


**Figure S2. Distribution of methylation scores (beta) based on probe type.** Histogram showing the distribution of methylation scores (*beta*, *x-axis*) across all sites included on the Illumina450K array prior to normalization. Red and blue bars represent Infinium I and II probe types respectively.

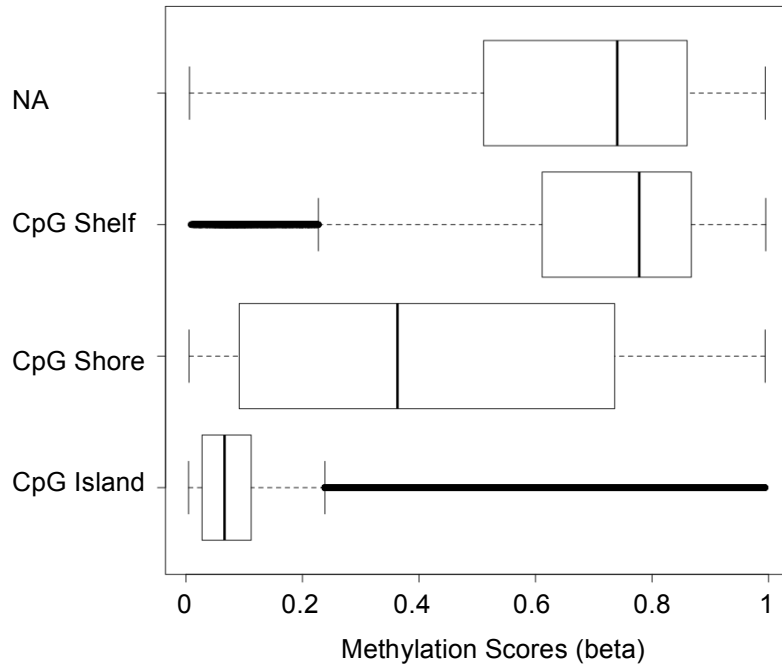


**Figure S3. DNA methylation profiles in CpG islands and surrounding regions.**

Methylation sites (N=344,403) were categorized in groups based on their location in CpG islands (*y-axis*) and plotted based on their methylation levels (*beta*, *x-axis*). The five-number summaries in the plot of each group represent the smallest observation, lower quartile, median, upper quartile, and largest observation (sample maximum). Ambiguous probes (i.e. probes falling in more than one category) were not included and NA denotes probes falling outside CpG Islands.

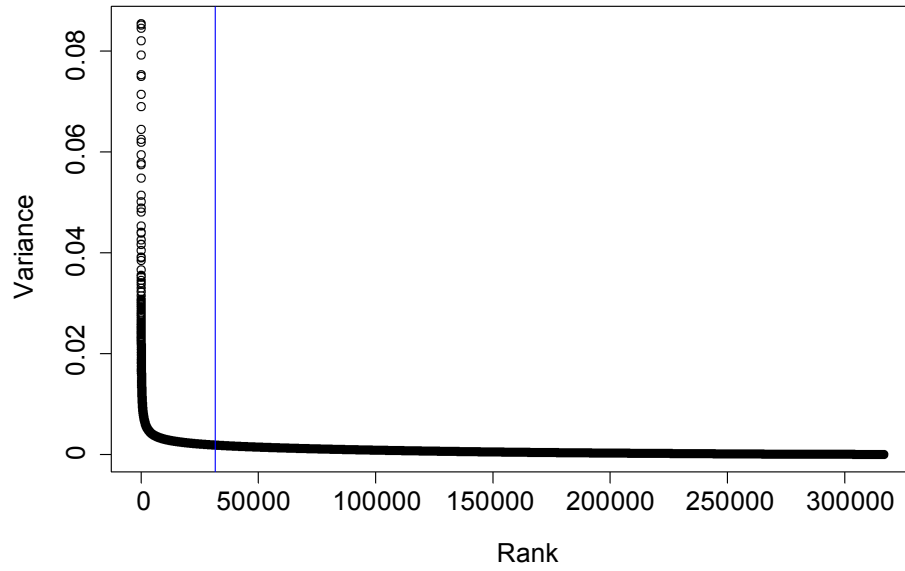


**Figure S4. Variance in DNA methylation levels (beta) across individuals.** Methylation sites (N=344,403) were ranked based on the variance in methylation beta levels across the 648 individuals and plotted in a scatterplot. The vertical blue line indicates the top 10% of the sites based on the variance.

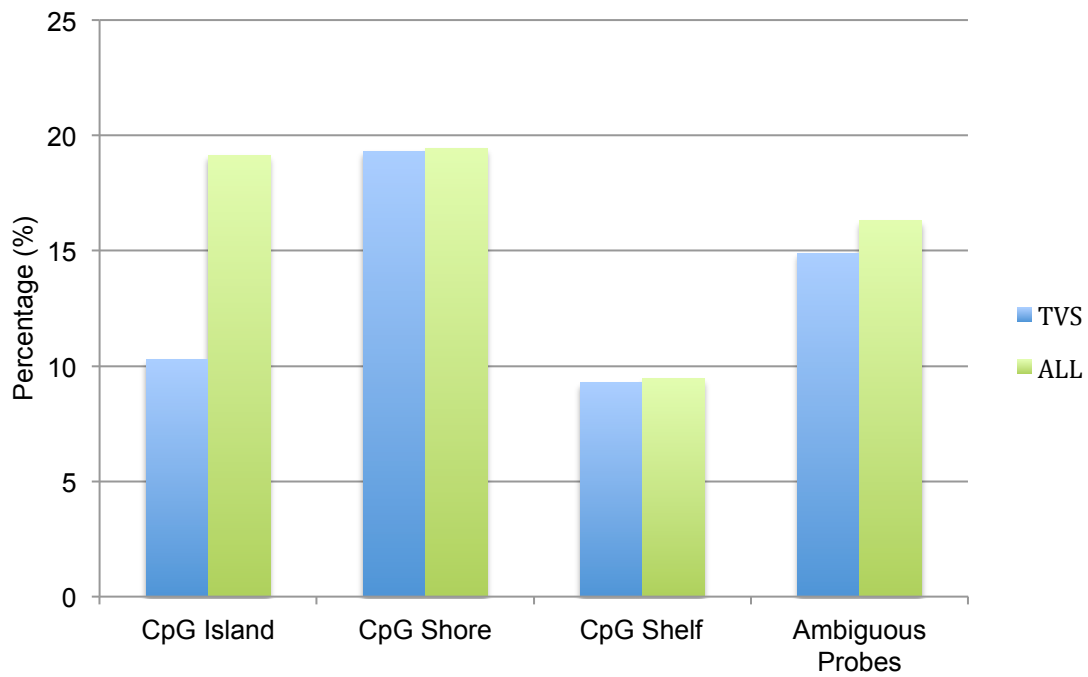


**Figure S5. Distribution of methylation sites based on location in CpG Islands and surrounding regions.** Methylation sites were categorized in groups based on their location (*x-axis*) in relation to CpG islands where sites that are 2kb away from the either side of a CpG Islands are considered to be shores and shelves are further 2kb away from either side of shores. Ambiguous sites refer to sites that fall in at least two different categories. TVS=Top variable (10%) sites and All=All mapped methylation sites (N=344,303)

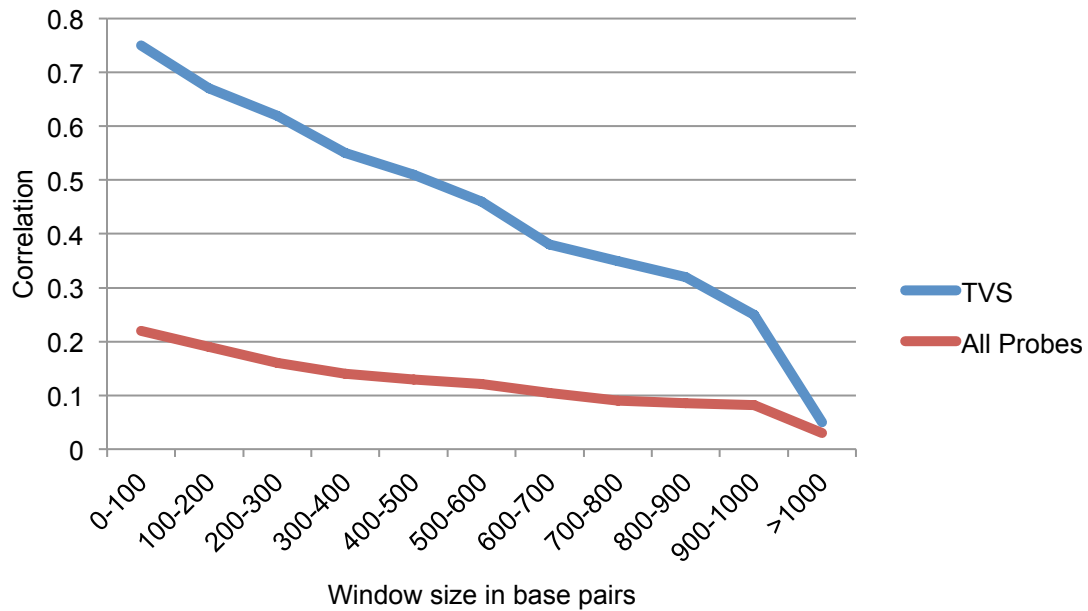


**Figure S6. Correlation of nearby methylation sites.** Pair-wise correlation of methylation sites located 0-1000bp apart with the y-axis indicating the average Spearman correlation coefficient ( $\rho$ ) of sites located in 100kb window categories (*x-axis*) for top variable sites (TVS) (N=34,430, blue line) and all sites (N = 344,303, red line).

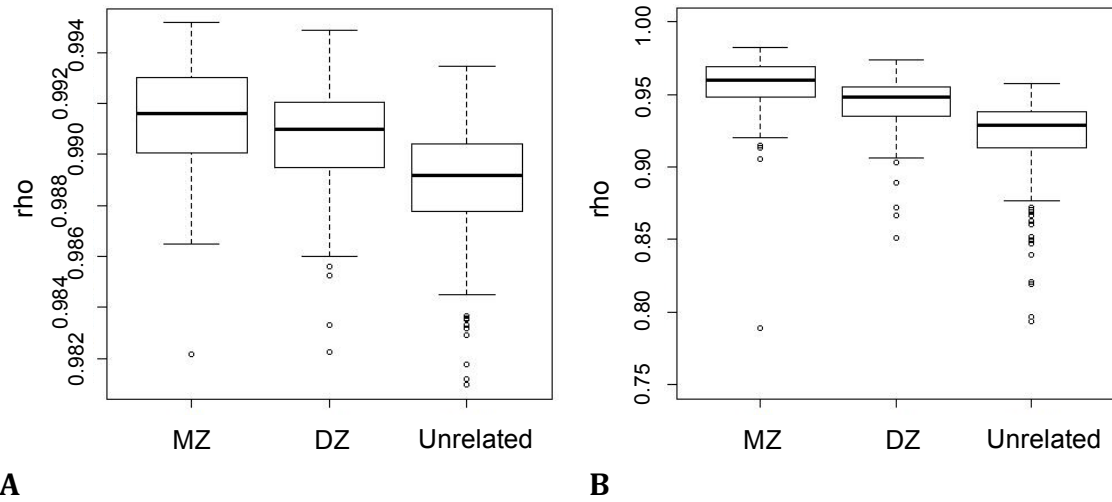


**Figure S7. Correlation of DNA methylation within and across twins.** Correlation of DNA methylation levels between all MZ co-twins, DZ co-twins and unrelated individuals were calculated using Spearman correlation analysis ( $\rho$ ,  $y$ -axis) and based on **(A)** all 344,303 probes as well as **(B)** restricted to TVS (N=34,430). The five-number summaries in each plot of each group represent the smallest observation, lower quartile, median, upper quartile, and largest observation (sample maximum)



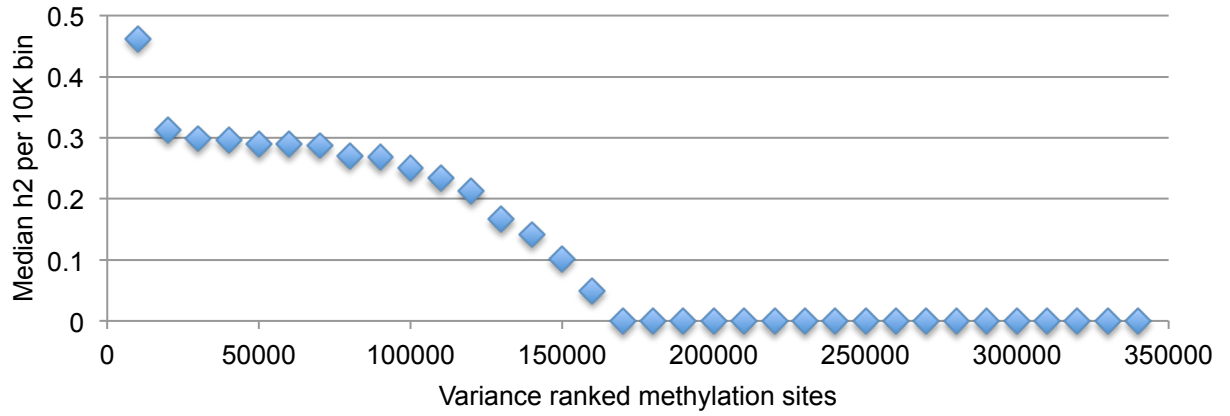
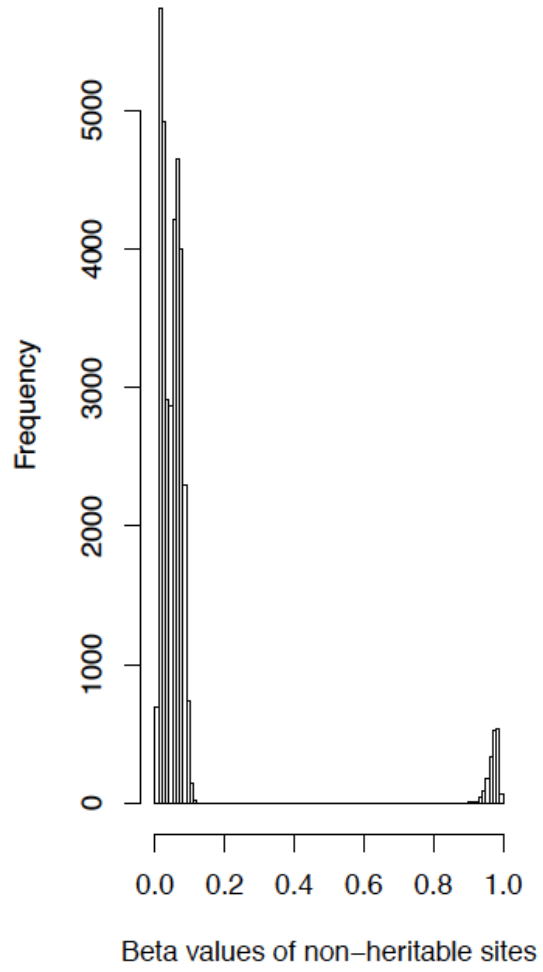
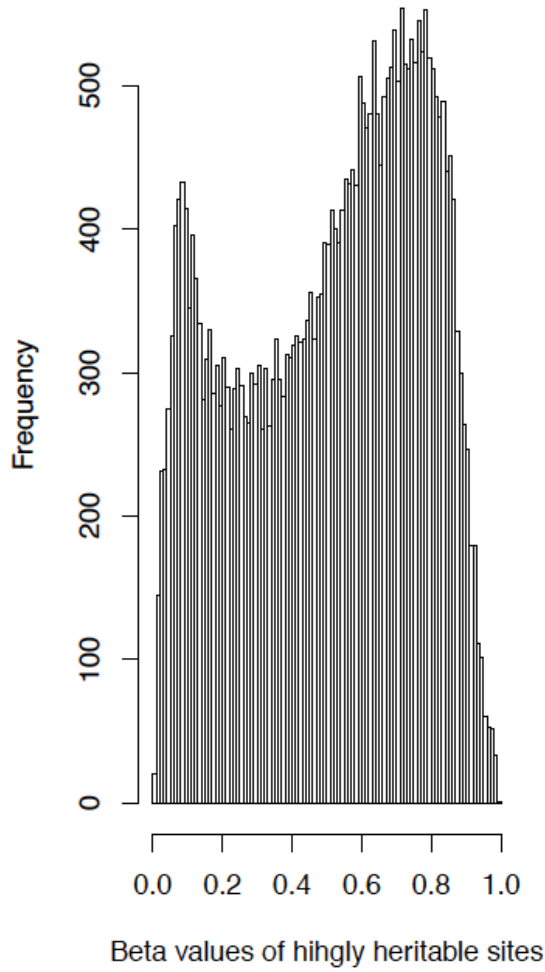
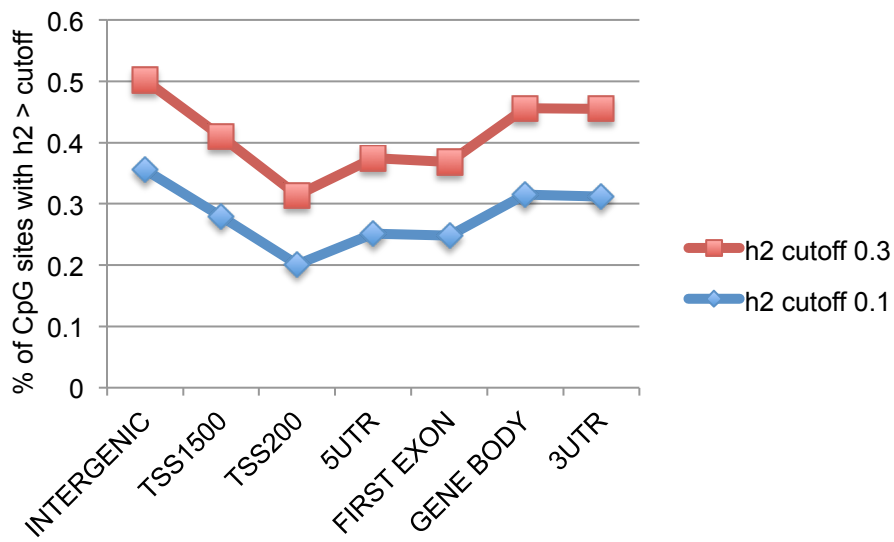


**Figure S8. Estimates of heritability based on population variation of methylation sites.** Methylation sites (N=344,092) were ranked based on the variance in beta levels across all individuals and binned in regions of 10,000 sites (*x-axis*). The median heritability ( $h^2$ , *y-axis*) estimates were calculated in each region and plotted.



**A**

**B**



**C**

**Figure S9. Characteristics of methylation sites dependent on heritability.**

(A) Top heritable sites ( $h^2 > 0.5$ ,  $N = 48072$ ) were profiled for their methylation levels and compared with (B) a set of similar sized non-heritable sites ( $h^2 \sim 0$ ). X-axes represent beta-values. (C) All methylation sites included in the heritability analysis ( $N = 344,092$ ) were categorized based on their genomic location where TSS1500 indicate sites located 200-1500bp upstream of TSS, TSS200 includes sites located 200bp upstream of TSS and intergenic refers to methylation sites not mapping in any of the other categories (x-axis). The proportion of methylation sites per category with  $h^2 > 0.1$  (blue line) or  $h^2 > 0.3$  (red line) were calculated and plotted accordingly (y-axis).

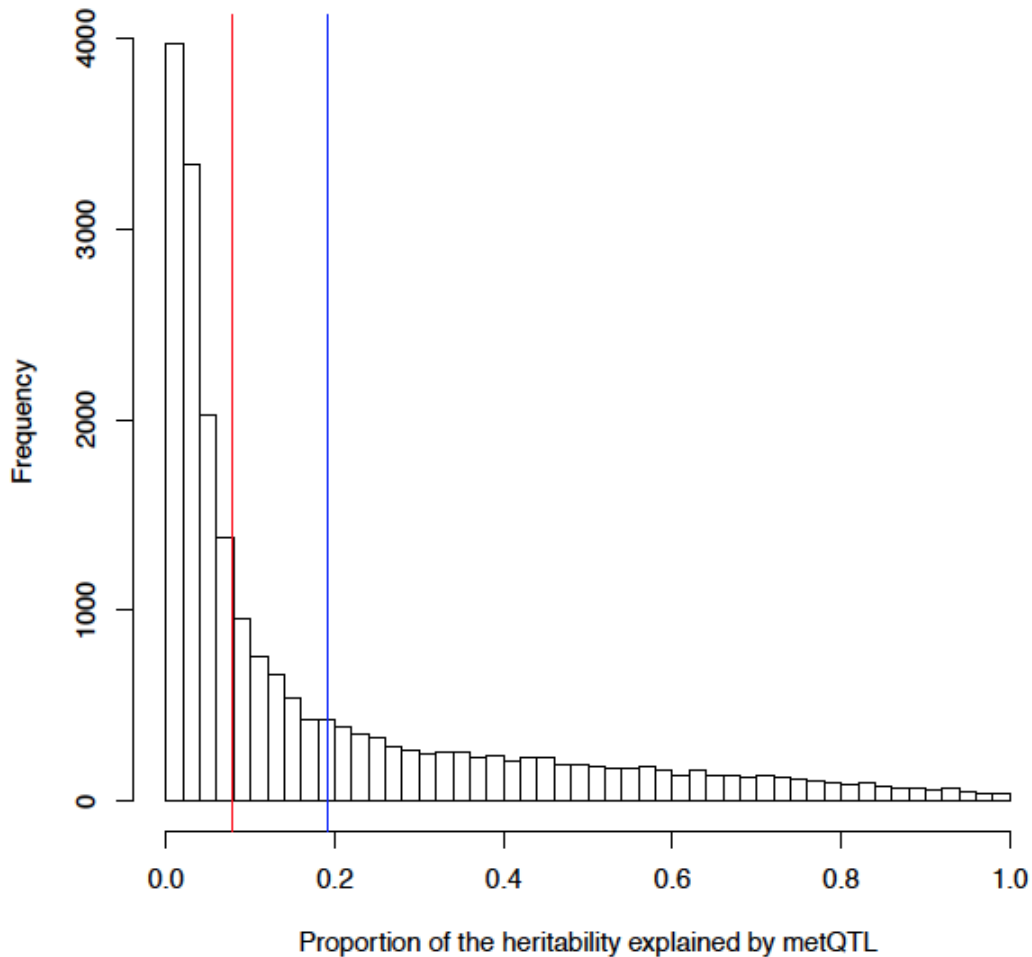


**Figure S10. The contribution of heritable *cis*-components to methylation variation.** Results from heritability ( $h^2$ ) and metQTL analyses ( $r^2$ ) were combined for the TVS with  $h^2 > 0.1$  ( $N = 21,144$ ) to generate proportion of the heritability that is explained by the significant metQTL (*cis*-SNP,  $MAF > 5\%$ ) (x-axis). Red line indicates median estimate (8%) and blue average, respectively (19%).

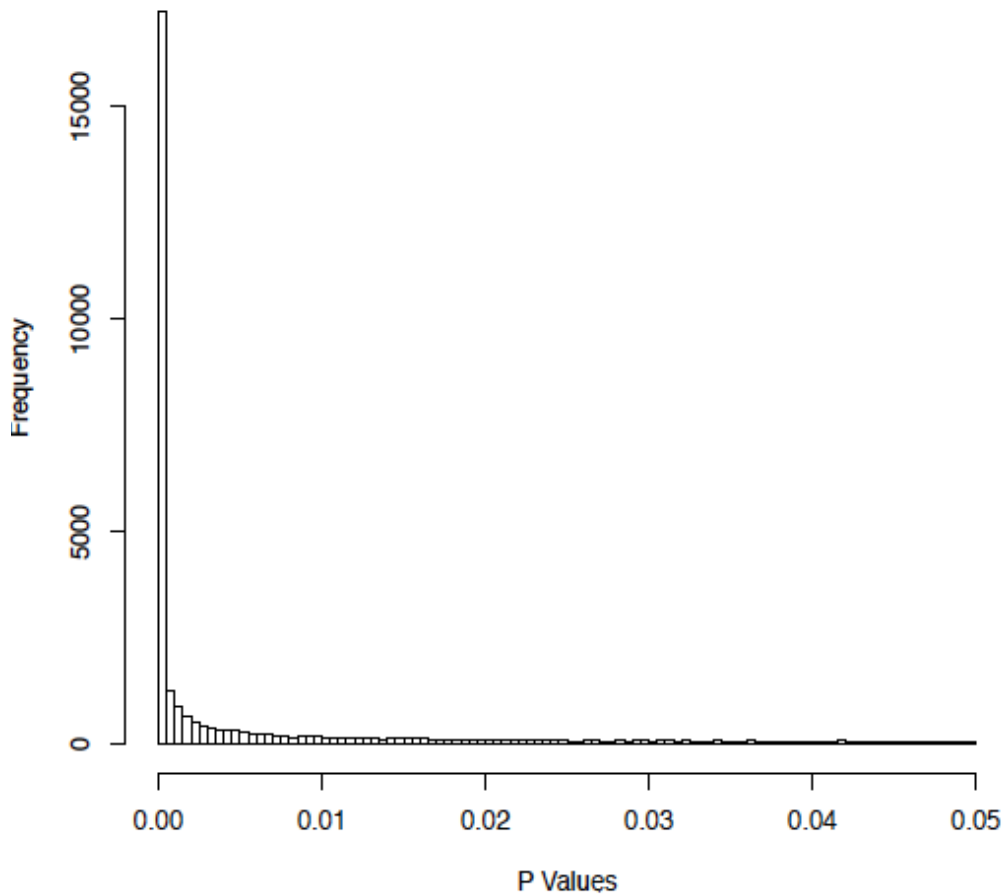
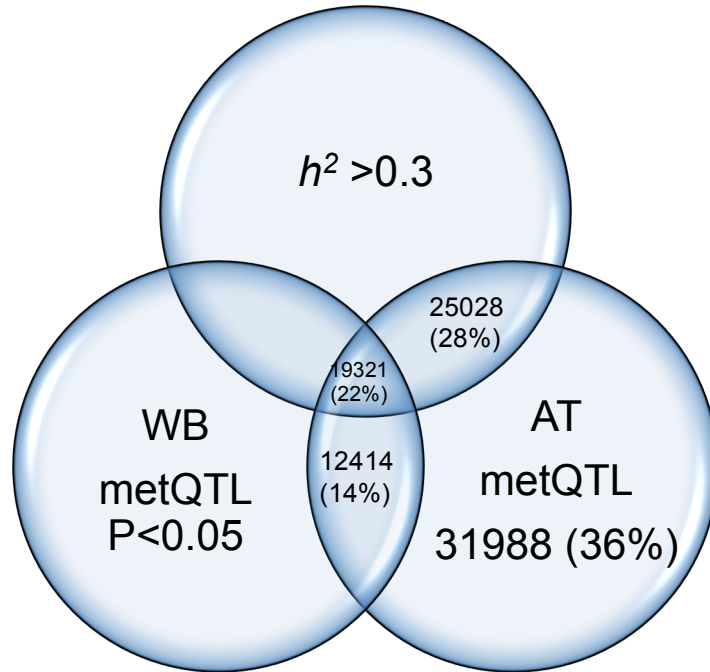
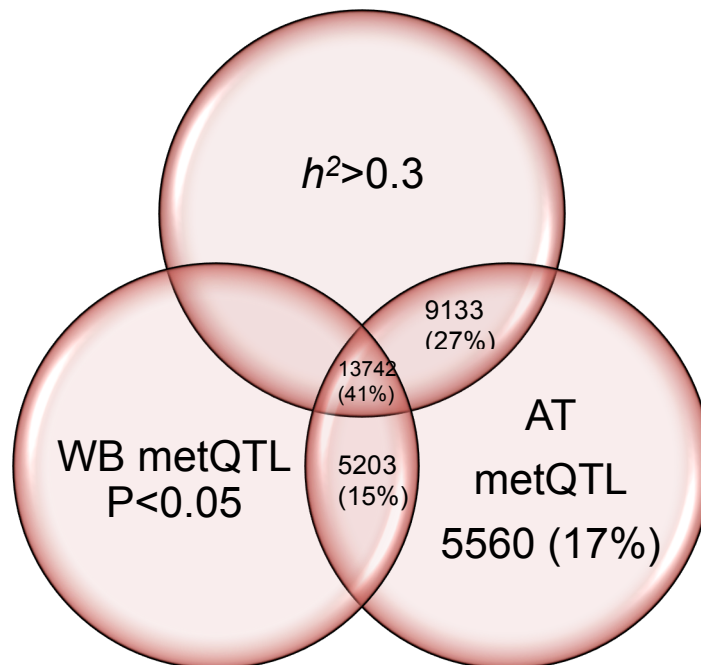


**Figure S11. Replication of metQTLs in whole blood samples.** Significant adipose metQTLs (FDR 1%) were validated in a set of whole-blood derived DNA samples profiled on the Illumina450K array. Histogram is showing P value distribution of significant ( $P < 0.05$ , same direction) associations identified in the replication cohort.



A



B

**Figure S12. Venn diagram** of adipose (AT) metQTL identified at FDR 1% (A) and Bonferroni corrected (B) and the overlap between highly heritable methylation sites ( $h^2 > 0.3$ ) and whole-blood (WB) metQTLs.

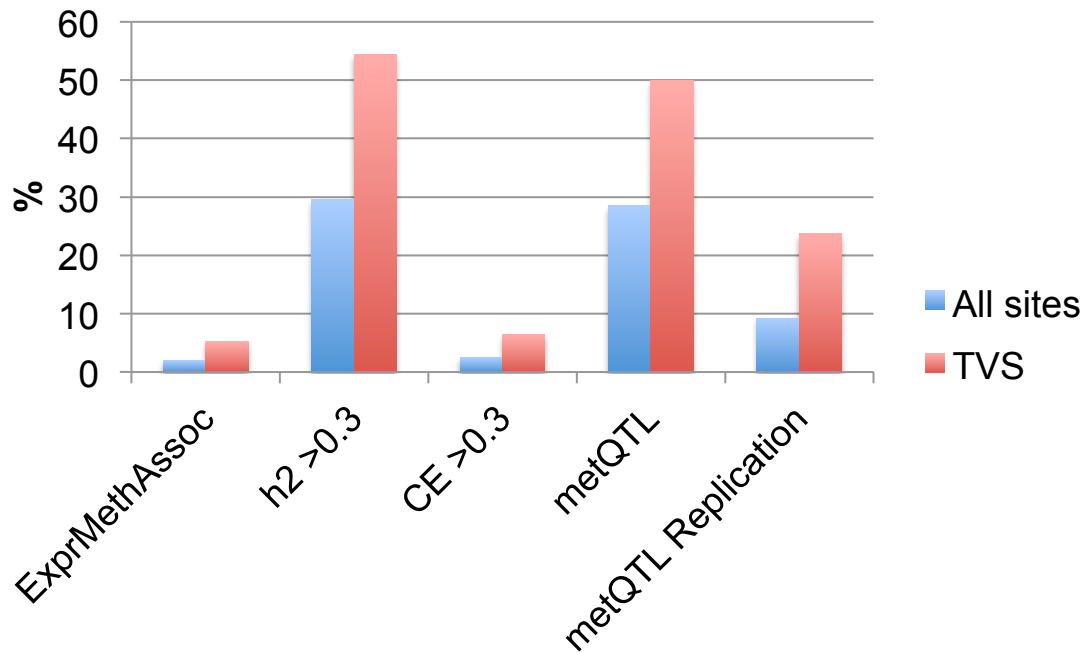


**Figure S13. Summary of the impact of variance in methylation levels on various analyses.** The proportion (*y-axis*) of significant associations between gene expression and DNA methylation (FDR 1%), highly heritable methylation sites ( $h^2 > 0.3$ ), methylation sites where common environment affects more than 30% of the overall methylation variance (CE  $> 0.3$ ), significant metQTLs (FDR1%) and metQTLs replicated in an independent tissue for all sites (blue bars) versus top variable sites (TVS, red bars).

**Table S8. Metabolic traits or diseases**

<b>Disease/trait</b>
Adiponectin levels
Body mass index
Cholesterol, total
HDL Cholesterol - Triglycerides (HDLC-TG)
Metabolic traits
Visceral fat
Obesity and osteoporosis
Obesity
Obesity (extreme)
Visceral adipose tissue/subcutaneous adipose tissue ratio
Triglycerides
HDL cholesterol
Visceral adipose tissue adjusted for BMI
Metabolite levels
Weight
Metabolic syndrome
Waist-hip ratio
Waist circumference
LDL cholesterol
Metabolic syndrome (bivariate traits)
Lipid metabolism phenotypes
Lipid levels in hepatitis C treatment
Adiposity